PROCEEDINGS OF SCIENCE

ONLINE ICRC 2021
THE ASTROPARTICLE PHYSICS CONFERENCE
Berlin | Germany
37th International Cosmic Ray Conference
12–23 July 2021

Particle escape from supernova remnants and related gamma-ray signatures

Silvia Celli[a,*] **and Giovanni Morlino**[b]

[a] *Dipartimento di Fisica dell'Università Sapienza di Roma and INFN-Sezione di Roma, P. le Aldo Moro 2, 00185, Rome, Italy,*
[b] *INAF, Osservatorio Astrofisico di Arcetri, L.go E. Fermi 5, Firenze, Italy*
E-mail: silvia.celli@roma1.infn.it, giovanni.morlino@inaf.it

The escape process of particles accelerated at supernova remnant (SNR) shocks is here studied with a phenomenological approach which allows to quantify its impact on the cosmic-ray (CR) spectrum observed on Earth, as well as on the gamma-ray spectral signatures emerging from these sources. Under the assumption that in the spatial region immediately outside of the remnant the diffusion coefficient is suppressed with respect to the average Galactic one, we show that a significant fraction of particles are still located inside the SNR long time after their nominal release from the acceleration region. This fact results into a gamma-ray spectrum arising from hadronic collisions that resembles a broken power law, similar to those observed in several middle-aged SNRs. Above the break, the spectral steepening is determined by the diffusion coefficient outside of the SNR and by the time dependence of maximum energy. The model of particles escape is also applied to electrons, including energy losses due to emission in radiation and magnetic fields of the region. Consequently, the comparison between the model prediction and broadband data allows to determine the model parameters which regulate both the energy-dependent escape process, as well as the particle propagation. We present the case of the Cygnus Loop SNR, where indeed the combination of radio and gamma-ray observations provides constraints on the efficiency of particle acceleration.

37th International Cosmic Ray Conference (ICRC 2021)
July 12th – 23rd, 2021
Online – Berlin, Germany

*Presenter

PoS(ICRC2021)924

1. Introduction

The process that allows CRs to escape from their sources and be released into the Galaxy is still largely unknown, mostly because its comprehension relies on details of the acceleration process and magnetic field evolution. Given the large uncertainties of current theoretical models [1, 2], here we adopt a phenomenological approach, consisting into a simplified description of the particle transport in spherical symmetry, capable of catching the particle decoupling from the SNR shock within a parametric description of the escape time [3]. In particular, a time-dependent solution for the density distribution of both protons and electrons is obtained. These solutions depend on the SNR temporal evolution, which is discussed in Sec. 2, and on the diffusive regime operating at the time when the particles start to escape the shock, whose details are provided in Sec. 3. Consequently, we derive the spectral energy density of the secondary gamma rays produced at the interaction between the accelerated protons and the target gas, as well as synchrotron and inverse Compton (IC) photons radiated by the electrons, in order to explore the possibility of constraining the regime of operation of particle escape by means of multi-wavelength observations. We apply the model to the broadband emission of the Cygnus Loop SNR in Sec. 4, highlighting the key role of gamma-ray data for constraining the particle escape. Conclusions are derived in Sec. 5.

2. The SNR dynamical evolution and the particle maximum energy

An SNR results from the interaction of ambient gas with stellar material ejected by a supernova (SN). The evolution of the interaction among the interstellar medium (ISM) gas and the ejecta can be characterized in terms of several distinct stages. While in the ejecta-dominated (ED) phase, the shock is almost in free-expansion, since the mass of the supernova (SN) ejecta $M_{\rm ej}$ dominates over the swept-up mass, later on the Sedov-Taylor (ST) phase onsets, and the expansion starts to become adiabatic, while radiative losses are still not significant. The transition time between these two stages is the so-called Sedov time, that for explosions occurring in a uniform environment of mass density ρ_0 reads as:

$$t_{\rm Sed} \simeq 1.6 \times 10^3 \ {\rm yr} \left(\frac{E_{\rm SN}}{10^{51} \ {\rm erg}}\right)^{-1/2} \left(\frac{M_{\rm ej}}{10 \, M\odot}\right)^{5/6} \left(\frac{\rho_0}{1 \, m_{\rm p}/{\rm cm}^3}\right)^{-1/3} , \quad (1)$$

where $m_{\rm p}$ is the proton mass, and $E_{\rm SN}$ is the kinetic energy released at the SN explosion. We refer to the analytical parametrization of [4] for the description of the temporal evolution of the shock radius $R_{\rm sh}$ and speed $u_{\rm sh}$ during the ED and ST stages, as well as along the transition.

The particle acceleration is believed to be highly efficient during the initial stages of the remnant evolution. A maximum value of the particle momentum $p_{\rm max}$, though not naturally embedded in the Diffusive Shock Acceleration (DSA) theory, is expected to exist in order to limit the spectral energy density of accelerated particles. However, a self-consistent description of the maximum energy achievable in the acceleration mechanism in a non-stationary framework requires the correct modeling of the evolution of the magnetic turbulence, which is supposed to be self-generated by the same accelerated particles, and possibly damped through frictional effects and wave cascade. Since such a complete description does not exist yet, we here use a quite general recipe, often adopted in the literature, which assumes that the maximum momentum increases with time during the ED phase, when the shock is actively accelerating particles, and then it decreases during the ST phase

according to a power law in time [see e.g. 5], namely:

$$p_{\rm max,0}(t) = \begin{cases} p_{\rm M}\,(t/t_{\rm Sed}) & \text{if } t \leqslant t_{\rm Sed} \\ p_{\rm M}\,(t/t_{\rm Sed})^{-\delta} & \text{if } t > t_{\rm Sed}\,, \end{cases} \tag{2}$$

where $p_{\rm M}$ represents the absolute maximum momentum, achieved at $t = t_{\rm Sed}$. Note that δ is a free parameter of the model, bounded to be positive, whose value strongly depends on the temporal evolution of the magnetic turbulence [3]. By inverting Eq. (2), we can also define the escape time for particles of given momentum p:

$$t_{\rm esc}(p) = t_{\rm Sed}\,(p/p_{\rm M})^{-1/\delta}\,, \tag{3}$$

corresponding to the time when these particles cannot be confined anymore by the turbulence and start escaping from the shock. It is also useful to define the escape radius as $R_{\rm esc}(p) = R_{\rm sh}\,(t_{\rm esc}(p))$. The onset of the escape process in the acceleration scenario introduces a unique feature in the evolution of the particle distribution, that will behave differently before and after $t_{\rm esc}(p)$. In fact, at times smaller than $t_{\rm esc}(p)$, particles closely follow the shock evolution as they are strictly tightened to the turbulence. On the other hand, at later times, when the turbulence starts to fade out, particles behave disconnected by the shock, and freely diffuse in the space. Particles evolving in these two regimes will be named respectively *confined particles* and *non-confined (or escaping) particles*.

3. Particle propagation in SNRs

The CR transport equation regulates the particle motion in the velocity and magnetic fields of the shock region and around. In the following Sec. 3.1 we will solve the transport equation for protons, which are subject to advection, diffusion and adiabatic losses, under the assumption that the internal structure of the moving plasma is such that its velocity profile is given by [6]

$$u(t,r) = \left(1 - \frac{1}{\sigma}\right)\frac{u_{\rm sh}(t)}{R_{\rm sh}(t)}r\,, \tag{4}$$

σ being the compression ratio at the shock ($\sigma = 4$ for strong shocks). Under this approximation, an analytical solution can be found for both the confined and the non-confined density function of protons during the ST evolutionary stage. In turn, the propagation of electrons is also affected by energy losses, as revealed by numerous observations of radiation spanning from radio to X rays in several SNRs [7], thus requiring the switch towards a numerical treatment for the solution of their transport equation, as discussed in Sec. 3.2.

Concerning that the efficiency in converting the shock bulk kinetic energy into relativistic particles, $\xi_{\rm CR}$, we assume that is constant in time, following [8]. The distribution function of CR accelerated at the shock is determined by DSA and it is predicted to be a featureless power law in momentum with slope α. In a simplified form, we write the particle spectrum at the shock as

$$f_0(t,p) = \frac{3\,\xi_{\rm CR}u_{\rm sh}^2(t)\rho_0}{4\pi\,c(m_{\rm p}c)^4\Lambda(p_{\rm max,0}(t))}\left(\frac{p}{m_{\rm p}c}\right)^{-\alpha}\Theta\left[p_{\rm max,0}(t) - p\right]\,, \tag{5}$$

where c is the speed of light. The spectral slope α is also a free parameter of the model. It is worth to recall, however, that DSA predicts α to be equal or very close to 4. Note that the function $\Lambda(p_{\rm max,0})$ is required to normalize the spectrum such that the CR pressure at the shock is $P_{\rm CR} = \xi_{\rm CR}\rho_0 u_{\rm sh}^2$.

3.1 Protons

The proton distribution function obeys the following equation:

$$\frac{\partial f}{\partial t} + u\frac{\partial f}{\partial r} = \frac{1}{r^2}\frac{\partial}{\partial r}\left[r^2 D\frac{\partial f}{\partial r}\right] + \frac{1}{r^2}\frac{\partial (r^2 u)}{\partial r}\frac{p}{3}\frac{\partial f}{\partial p}\,, \tag{6}$$

where the effective spatial diffusion coefficient experienced by particles is indicated with $D(t, r, p)$. The simplified transport equation for the confined particle density function $f_{\rm conf}$ reads as:

$$\frac{\partial f_{\rm conf}}{\partial t} + u\frac{\partial f_{\rm conf}}{\partial r} = \frac{1}{r^2}\frac{\partial (r^2 u)}{\partial r}\frac{p}{3}\frac{\partial f_{\rm conf}}{\partial p}\,. \tag{7}$$

where we assume that diffusion inside the SNR is strongly suppressed, such that advection dominates the particle transport for $t < t_{\rm esc}(p)$. In order to describe the particle evolution at early times after the escape, namely for $t > t_{\rm esc}(p)$, an approximate solution is obtained by assuming that particles decouple from the SNR and their evolution is governed by pure diffusion. The particle density evolution is hence described by the same Eq. (6) but dropping the terms including u, which gives:

$$\frac{\partial f_{\rm esc}}{\partial t} = \frac{1}{r^2}\frac{\partial}{\partial r}\left[r^2 D(p)\frac{\partial f_{\rm esc}}{\partial r}\right]\,, \tag{8}$$

where from now on we will address $f_{\rm esc}(t, r, p)$ as the distribution of non-confined particles. Note that the diffusion coefficient is here assumed spatially homogeneous and stationary, as to allow an analytic solution. Unless specified differently, we will consider it Kolmogorov-like, namely

$$D(p) \equiv \chi D_{\rm Gal}(p) = \chi 10^{28}\left(\frac{pc}{10\,{\rm GeV}}\right)^{1/3}\,{\rm cm^2\,s^{-1}}\,, \tag{9}$$

where the parameter χ quantifies the difference with respect to the average Galactic diffusion coefficient. Since the particles will start escaping after they have been confined by the turbulence, this equation will be solved with an initial condition given by the distribution function of confined particles at $t = t_{\rm esc}(p)$. We refer to [3] for details on the methods and the analytic solutions of the particle density in the two different propagation regimes, obtained for acceleration spectra with either $\alpha = 4$ or $\alpha = 4 + 1/3$ (see Eq. (5)).

3.2 Electrons

In order to evaluate the impact on the electron spectrum of energy losses as a function of time, we need to estimate the magnetic field strength at the shock, and its evolution in the remnant interior while it is expanding. The value of the magnetic field at the shock is the result of both amplification, that we here account for parametrically as due to proton-self amplification, and compression at the shock of the circumstellar magnetic field. The former is connected to the maximum energy of protons, as given by Eq. (2). Assuming that $p_{\rm max,0}(t)$ is determined by the age-limited condition $t_{\rm acc} = t_{\rm SNR}$, we can derive the magnetic field using the acceleration time $t_{\rm acc} \simeq 8D_1(p)/u_{\rm sh}^2$ where the upstream diffusion coefficient is $D_1(p) = D_B/\mathcal{F}$, D_B being the Bohm diffusion coefficient and $\mathcal{F}$ the magnetic logarithmic power spectrum. Note that we will use the subscript 1 (2) for the quantities calculated in the upstream (downstream). Because of Eq. (2), we get

$$\mathcal{F}(t) = \frac{8\,p_{\rm M}c}{3\,eB_0\,c\,t_{\rm Sed}}\begin{cases}\left(\frac{u_{\rm sh}}{c}\right)^{-2} & t < t_{\rm Sed}\\ \left(\frac{u_{\rm sh}}{c}\right)^{-2}\left(\frac{t}{t_{\rm Sed}}\right)^{-\delta-1} & t \geq t_{\rm Sed}\,,\end{cases} \tag{10}$$

where B_0 is the upstream ordered magnetic field. Assuming the empirical formula $\mathcal{F}^{-1} = (B_0/\delta B) + (B_0/\delta B)^2$, the turbulent component of the upstream magnetic field is then

$$\delta B_1(t) = \frac{B_0}{2}\left(\mathcal{F}(t) + \sqrt{4\mathcal{F}(t) + \mathcal{F}^2(t)}\right), \tag{11}$$

such that the total magnetic field strength in the shock upstream is then $B_{1,\rm tot}(t) = \left(B_0^2 + \delta B_1^2(t)\right)^{1/2}$. Crossing the shock towards downstream, the magnetic field is further compressed by a factor $r_{\rm B} = \sqrt{11}$ for a randomly oriented field. As a result, the downstream total field at the shock position is equal to $B_{2,\rm tot}(t) = r_{\rm B} B_{1,\rm tot}(t)$. In addition to field compression, the evolution of the downstream field is further affected by adiabatic losses. In the assumption of an isotropic magnetic field, the ordered component gets diluted with position within the shock radius and time as [13]

$$B_2^2(r,t) = \frac{B_0^2}{3}\left[\left(\frac{R_{\rm sh}(t)}{r}\right)^4 + 2\sigma^2 L^6(t',t)\left(\frac{R_{\rm sh}(t)}{r}\right)^2\right], \tag{12}$$

where $t'(t,r)$ indicates the time when the plasma located at time t in position r was shocked [3]. Neglecting damping effects, a similar expression can be written for the downstream turbulent component, substituting in the LHS B_2 with δB_2 and in the RHS B_0 with δB_1. The factor $L(t',t)$ in Eq. (12) accounts for adiabatic losses that the magnetic field undergoes in the time interval $t - t'$:

$$L(t',t) = \left[\frac{\rho_2(t,r)}{\rho_2(t'(t,r))}\right]^{1/3} \implies L(t',t) = \left[\frac{R_{\rm sh}(t')}{R_{\rm sh}(t)}\right]^{3/4} \tag{13}$$

where $\rho_2(t',r)$ is the density of the downstream (shoked) plasma element right at the time it was shocked, i.e. $t'(t,r)$. The factor $L(t',t) \leq 1$. Note that particles are subject to the same losses. To compute the adiabatic factor in the last equality, we made use of its dependence on the shock radius.

The instantaneous electron spectrum at the shock, $f_{\rm e,0}(p)$, is assumed proportional to the proton spectrum, $f_0(p)$. Nonetheless, its cutoff is located at the maximum energy which is determined by the condition $t_{\rm acc} = \min[t_{\rm SNR}, \tau_{\rm loss}]$, namely acceleration time either limited by SNR age of by loss time. In the loss dominated case, a super-exponential cutoff is present [9, 10]. In particular, when energy losses are proportional to E^2, like in the case of synchrotron and inverse Compton processes, the cutoff is $\propto \exp\left[-(p/p_{{\rm max},e})^2\right]$, holding in the loss-dominated scenario. A good approximation to the spectrum of electrons is provided by:

$$f_{e,0}(p) = K_{\rm ep}\, f_0(p)\left[1 + 0.523\left(p/p_{\rm max,e}\right)^{\frac{9}{4}}\right]^2 e^{-\left(\frac{p}{p_{\rm max,e}}\right)^2}. \tag{14}$$

The factor $K_{\rm ep}$ accounts for the different normalization between electrons and protons, which is likely related to the different mechanisms responsible for lepton and hadron injection [11]. In turn, the electron maximum energy, as limited by energy losses, can be estimated starting from the energy loss rate due to synchrotron plus IC scattering, which is

$$\left(\frac{{\rm d}E}{{\rm d}t}\right)_{\rm syn+IC} = -\frac{\sigma_{\rm T} c}{6\pi}\left(\frac{E}{m_{\rm e}c^2}\right)^2\left(B^2 + B_{\rm eq}^2\right), \tag{15}$$

where $\sigma_{\rm T}$ is the Thomson cross section and $m_{\rm e}$ the mass of the electron, while $B_{\rm eq}^2 = 8\pi U_{\rm rad}$ is the equivalent magnetic field associated to the interstellar radiation field of energy density

$U_{\rm rad}$. Imposing the condition $t_{\rm acc} = \tau_{\rm loss}$ ($\tau_{\rm loss}$ being the total loss timescale calculated from the synchrotron + IC losses, averaged over the time spent upstream and downstream of the shock) we get the following expression for the maximum energy:

$$\frac{E_{\rm max,e}(t)}{m_e c^2} = \sqrt{\frac{(\sigma-1) r_{\rm B}}{\sigma\left[r_{\rm B}(1+\sigma_{\rm eq}^2)+\sigma(r_{\rm B}^2+\sigma_{\rm eq}^2)\right]}\frac{6\pi e B_0 \mathcal{F}(t)}{\sigma_{\rm T} B_{1,\rm tot}^2(t)}}\,\frac{u_{\rm sh}(t)}{c}\,, \tag{16}$$

where $\sigma_{\rm eq} = B_{\rm eq}/B_{1,\rm tot}$. Once the electron spectrum at the shock is known (see Eq. (14)), we can proceed to derive the downstream particle distribution function, by solving the temporal evolution of the particle energy with loss terms due to adiabatic expansion and radiative processes [12]

$$\frac{{\rm d}E}{{\rm d}t} = \left(\frac{{\rm d}E}{{\rm d}t}\right)_{\rm syn+IC} + \frac{E}{L}\frac{{\rm d}L}{{\rm d}t}\,, \tag{17}$$

where L is the adiabatic loss function, given in Eq. (13). Because of energy losses, electrons produced at time t' with energy E' will thus have an energy $E(t)$ at a later time t given by [13]:

$$\frac{E(t)}{E'} = \frac{L(t',t)}{1 + A\,E'\int_{t'}^{t} L(t',\tau)\left[B_{2,\rm tot}^2(\tau) + B_{\rm eq}^2\right]{\rm d}\tau}\,, \tag{18}$$

where $A = \sigma_{\rm T} c/(6\pi m_{\rm e}^2 c^4)$. By imposing number conservation and defining the quantity $I(t',t) = A\int_{t'}^{t} L(t',\tau)\left[B_{2,\rm tot}^2(\tau) + B_{\rm eq}^2\right] d\tau$, the electron spectrum at time t results to be:

$$f_{e,\rm conf}(E,r,t) = f_{e,0}\left(\frac{E}{L(t',t) - IE}, t'\right)\frac{L^4}{(L-IE)^2}\,. \tag{19}$$

4. The Cygnus Loop SNR

The Cygnus Loop is a bright SNR, located at an estimated distance of ~ 735 pc, whose age is supposed to amount to $\sim 2\times10^4$ yr. It presents a complex morphology, which deviates largely from its classification of typical middle-aged shell-type SNR. In radio [15], two prominent shells (NGC 6960 and NGC 6992) and a central filament emerge. NGC 6992, likely governed by the interaction of the SNR blast wave with clouds, is also the brightest sector of the gamma-ray Cygnus Loop emission observed with Fermi-LAT between 1 and 100 GeV [14]. Our modeling of the non-thermal radiation from the entire SNR accounts for several mechanisms, including proton collisions on target gas density (pp interaction), electron IC scattering on background photons (CMB, UV, optical and IR), and synchrotron emission from electrons in the SNR magnetic field [15], each resulting from both confined and escaping particles. In addition to these, radiation from the region of the precursor is also included, producing a flattening of the particle spectra towards the largest energies, where particles do not suffer adiabatic losses. In the following, we outline how data constrain each single parameter of the model. In order to match the present values of the shock radius and speed, $M_{\rm ej} = 5M_\odot$ and $E_{\rm SN} = 7\times10^{50}$ erg are assumed in the following. The radio spectral index s fixes the particle spectral slope through the relation $\alpha = 2s+3$, hence $s \simeq 0.5 \implies \alpha \simeq 4$, in good agreement with linear DSA prediction. As the observed gamma-ray spectrum is expected to arise entirely though pp collisions, its normalization allows us to fix the acceleration efficiency $\xi_{\rm CR}$,

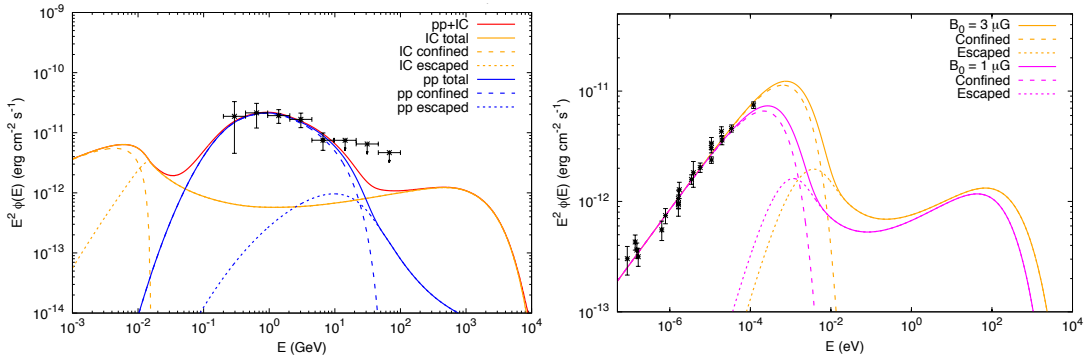

(a) (b)

Figure 1: Left: Gamma-ray emission predicted from the model compared with Fermi-LAT data [14]. Hadronic (pp) and leptonic (IC) components are shown respectively with blue and yellow lines, their sum being in red. **Right:** Synchrotron emission derived from the model compared with radio data from the whole SNR [15]. Yellow lines show our best model, assuming $B_0 = 3\,\mu$G, as well as the case with $B_0 = 1\,\mu$G in magenta. Dashed and dotted lines refer to the contribution from confined and escaped particles, respectively. Figure reproduced from [15], under the CC BY license.

once the target density is fixed: for $n_0 = 0.4$ cm^{-3}, we derive $\xi_{\rm CR} = 7\%$. On the other hand, the spectral shape beyond few GeV simultaneously constraints $p_{\rm M}, \delta$ and χ. Unfortunately, the lacks data beyond a few 10 GeV results in some degeneracy between those three parameters. Hence, we make the conservative assumption $D = D_{\rm Gal}$, which allows us to constrain $p_{\rm M} \simeq 200$ TeV and $\delta \simeq 3$ in order to reproduce the gamma-ray data as shown in Fig. 1(a). It is worth stressing that the IC emission spectrum from escaping electrons is quite flat and dominates the emission above ~ 30 GeV. Even if those electrons have been accelerated in the past, a fraction of them is still located inside the SNR and its amount depends on the diffusion coefficient like $N \propto D^{-3/2}$. As a consequence, $\chi = 1$ should be considered as a lower limit, in that $\chi \ll 1$ would result in overshooting the Fermi-LAT upper limits above 10 GeV. An interesting test for our model would be to look for the TeV emission produced through IC by escaping electrons. The differential flux at 1 TeV is $\sim 10^{-12}$ erg s^{-1} cm^{-2}, well within the sensitivity range of current imaging atmospheric Cherenkov telescopes (IACTs). Unfortunately, the Cygnus Loop is very extended, what makes the observation very challenging for the limited field of view. An attempt was made by the MAGIC collaboration, resulting only in upper limits (compatible with our predictions). The large IC flux produced by the escaping electrons in the gamma-ray band results from the large electron density as inferred from the radio data. In fact, radio data allow to estimate the remaining parameters, $K_{\rm ep}$ and B_0, which are 0.15 and 3 μG, respectively, for our fiducial model shown in Fig. 1(b). In particular, the magnetic field is determined by the absence of any spectral break up to the highest frequency point detected by Planck at 30 GHz. For our fiducial model the breaking frequency is located at ~ 200 GHz and below such energy the emission behaves like a single power-law.

5. Conclusions

By modeling the radio and gamma-ray emission of the Cygnus Loop in the context of particle propagation and escape from a middle-aged SNR, we constrained the nowadays maximum particle

energy (for both electrons and protons) at 65 GeV, and the magnetic field strength at the shock at 10 μG. We also constrain the temporal behavior of maximum accelerated energy, suggesting the existence of magnetic field amplification at the shock. In addition, the model description of the radio also constrains the electron density, revealing a dominant IC emission from escaping electrons in the gamma-ray spectrum above $\sim$ 10 GeV. This result sheds new light on the electron contribution to the SNR spectral features at high energies. In this respect, future gamma-ray observations with the next IACT generation, like the Cherenkov Telescope Array (CTA), could be crucial to investigate the emission produced through IC by escaping electrons at energies $\sim$ 1 TeV and place observing constraints on this spectral tendency.

References

[1] M. A. Malkov et al., *Analytic solution for self-regulated collective escape of cosmic rays from their acceleration sites*, ApJ **768** (2013) 73, arXiv:1207.4728;

[2] L. Nava et al., *Non-linear diffusion of cosmic rays escaping from supernova remnants - I. The effect of neutrals*, MNRAS **461** (2016) 3552, arXiv:1606.06902;

[3] S. Celli et al., *Exploring particle escape in supernova remnants through gamma rays*, MNRAS **490** 4317 (2019), arXiv:1906.09454;

[4] J. K. Truelove and C. F. McKee, *Evolution of Nonradiative Supernova Remnants*, ApJS **120** (1999) 299;

[5] S. Gabici et al., *Broad-band non-thermal emission from molecular clouds illuminated by cosmic rays from nearby supernova remnants*, MNRAS **396** (2009) 1629, arXiv:0901.4549;

[6] J. P. Ostriker and C. F. McKee, *Astrophysical blastwaves*, Reviews of Modern Physics **60** (1988) 1;

[7] J. Vink, *Supernova remnants: the X-ray perspective*, A&ARv **20** (2012) 49, arXiv:1112.0576;

[8] V. S. Ptuskin and V. N. Zirakashvili, *On the spectrum of high-energy cosmic rays produced by supernova remnants in the presence of strong cosmic-ray streaming instability and wave dissipation*, A&A **429** (2005) 755, arXiv:astro-ph/0408025;

[9] V. N. Zirakashvili and F. A. Aharonian, *Analytical solutions for energy spectra of electrons accelerated by nonrelativistic shock-waves in shell type supernova remnants*, A&A **465** (2007) 695, arXiv:astro-ph/0612717;

[10] P. Blasi, *Shock acceleration of electrons in the presence of synchrotron losses - I. Test-particle theory*, MNRAS **402** (2010) 2807B, arXiv:0912.2053;

[11] G. Morlino and S. Celli, *Cosmic-ray electrons released by supernova remnants*, submitted to MNRAS (2021), arXiv:2106.06488;

[12] G. Morlino and D. Caprioli, *Strong evidence for hadron acceleration in Tycho's supernova remnant*, A&A **538** (2012) A81, arXiv:1105.6342;

[13] S. P. Reynolds, *Models of Synchrotron X-Rays from Shell Supernova Remnants*, ApJ **493** (1998) 375;

[14] H. Katagiri et al., *Fermi Large Area Telescope observations of the Cygnus Loop supernova remnant*, ApJ **741** (2011) 44, arXiv:1108.1833;

[15] S. Loru et al., *New high-frequency radio observations of the Cygnus Loop supernova remnant with the Italian radio telescopes*, MNRAS **500** (2020) 5177, arXiv:2009.09948.